

RESEARCH

Open Access



Analysis of the materials and processes of hanging sculptures in Guanyin Hall

Bochao Zhong¹, Chengquan Qiao¹, Dongyoung Yoo¹, Decai Gong¹ and Yuxuan Gong^{2*}

Abstract

Changzhi Guanyin Hall, a folk temple from the Ming Dynasty, embodies the essence of the 'unity of the three religions' philosophy, centred around Guanyin Bodhisattva. Over 500 sculptures reside within a modest 70 m² space, encompassing representations from Confucianism, Buddhism and Taoism. Ranging from a towering 2 m to a mere 10 cm, these sculptures depict an array of characters and mythological scenes, bestowing considerable importance upon the painted sculptures of Guanyin Hall. Varying degrees of deterioration have affected these sculptures due to the passage of time and suboptimal preservation conditions, highlighting the imperative need for meticulous restoration efforts. However, the absence of comprehensive analyses pertaining to the production process of Guanyin Hall sculptures has hindered the restoration groundwork. This study focuses on fallen hanging sculptures and debris, encompassing intact sculptures, clay fragments, wooden sticks, plant fibres, wires and pigments. Employing a series of techniques, including X-ray photography, microscopic analysis, mineral analysis (MLA), laser particle size testing, ion chromatography, X-ray fluorescence spectroscopy (XRF), X-ray diffractometer (XRD) and energy dispersive spectrometer (SEM–EDS) analysis, this research characterises the constituent materials used in crafting these artifacts. Instead of a full-body skeleton, the findings reveal that the small hanging sculpture is supported by delicate wires that hold specific areas, such as the arms and the gown hems. The hanging sculptures are made from a single type of clay and are reinforced with either mulberry bast or wheat straw fibres. A Pinaceae wood stick affixes the head to the body, and the sculpture is then suspended on the wall through nails inserted into the feet. The moulded clay undergoes a sequence of carving, drying and polishing and is coated with a white ash layer before receiving intricate painting. Mineral pigments, including cinnabar, red lead, iron red, cerussite, atacamite, brochantite and azurite, adorn the surface of the sculptures, with gold foil embellishing the golden elements. The intricate artisanry and multifaceted material composition of Guanyin Hall's painted sculptures render them unparalleled artistic treasures, not solely within Shanxi but across the entire nation. Furthermore, this study establishes a dependable foundation for conservation and restoration endeavours.

Keywords Guanyin Hall, Painted sculpture, Production process, Material analysis, Clay sculpture conservation

Introduction

Guanyin Hall, situated in the northwest suburb of Changzhi City, Shanxi Province, near Liangjiazhuang Village, was constructed during the 10th year of the Wanli era in the Ming Dynasty (A.D. 1582). The architectural layout comprises two courtyards, aligned from east to west, featuring the Theater Building (first gate) along the central axis, followed by the Heavenly King Hall (second gate), culminating in the Guanyin Hall. Serving as the principal hall of Guanyin Temple, Guanyin Hall accommodates

*Correspondence:

Yuxuan Gong
gongyuxuan@hotmail.com

¹ Department for the History of Science and Scientific Archaeology, University of Science and Technology of China, 96 Jinzhai Rd, Hefei, People's Republic of China

² Department for the History of Science, Jiangsu University of Science and Technology, 666 Changhui Rd, Zhenjiang, People's Republic of China
Full list of author information is available at the end of the article



© The Author(s) 2023. **Open Access** This article is licensed under a Creative Commons Attribution 4.0 International License, which permits use, sharing, adaptation, distribution and reproduction in any medium or format, as long as you give appropriate credit to the original author(s) and the source, provide a link to the Creative Commons licence, and indicate if changes were made. The images or other third party material in this article are included in the article's Creative Commons licence, unless indicated otherwise in a credit line to the material. If material is not included in the article's Creative Commons licence and your intended use is not permitted by statutory regulation or exceeds the permitted use, you will need to obtain permission directly from the copyright holder. To view a copy of this licence, visit <http://creativecommons.org/licenses/by/4.0/>. The Creative Commons Public Domain Dedication waiver (<http://creativecommons.org/publicdomain/zero/1.0/>) applies to the data made available in this article, unless otherwise stated in a credit line to the data.

a total of 562 painted sculptures, encompassing figures from Confucianism, Buddhism and Taoism. Alongside these figures, embellishments such as buildings, auspicious creatures, celestial clouds and flora intertwine, reenacting a myriad of scenes from timeless mythological narratives [1]. The painted sculptures within Guanyin Hall represent a valuable historical resource for the exploration of painted sculpture artifacts, art history and folk culture. Their substantial historical, artistic and scientific importance prompted the designation of Guanyin Hall as a Key Cultural Relics Site under State Protection in 2001. More than 13,000 painted clay sculptures exist in Shanxi, spanning more than 1000 years in eight eras from the Tang to the Qing Dynasty, which are unique in terms of quantity and preciousness. The development of traditional handicrafts and religions in Shanxi was less influenced by changing times due to the relatively closed

geographical environment and simple folk culture, gradually gathering numerous excellent painters and craftsmen. Consequently, a rich variety of folk arts have been inherited and developed in this region, of which Changzhi Guanyin Hall is a representative. Compared with the temples built by the ancient officials, Guanyin Hall is closer to the folk and emphasises the concept of humanity [2].

Two primary categories of Guanyin Hall sculptures exist: placement and hanging sculptures. Notably, the three central sculptures of the east wall and those on the first, second and third levels of the north and south walls are placement sculptures, whereas smaller sculptures situated at greater heights assume the form of hanging sculptures [3], as illustrated in Fig. 1. Placement sculptures, characterised by their medium-to-large dimensions, either detach from the wall surface or rely on

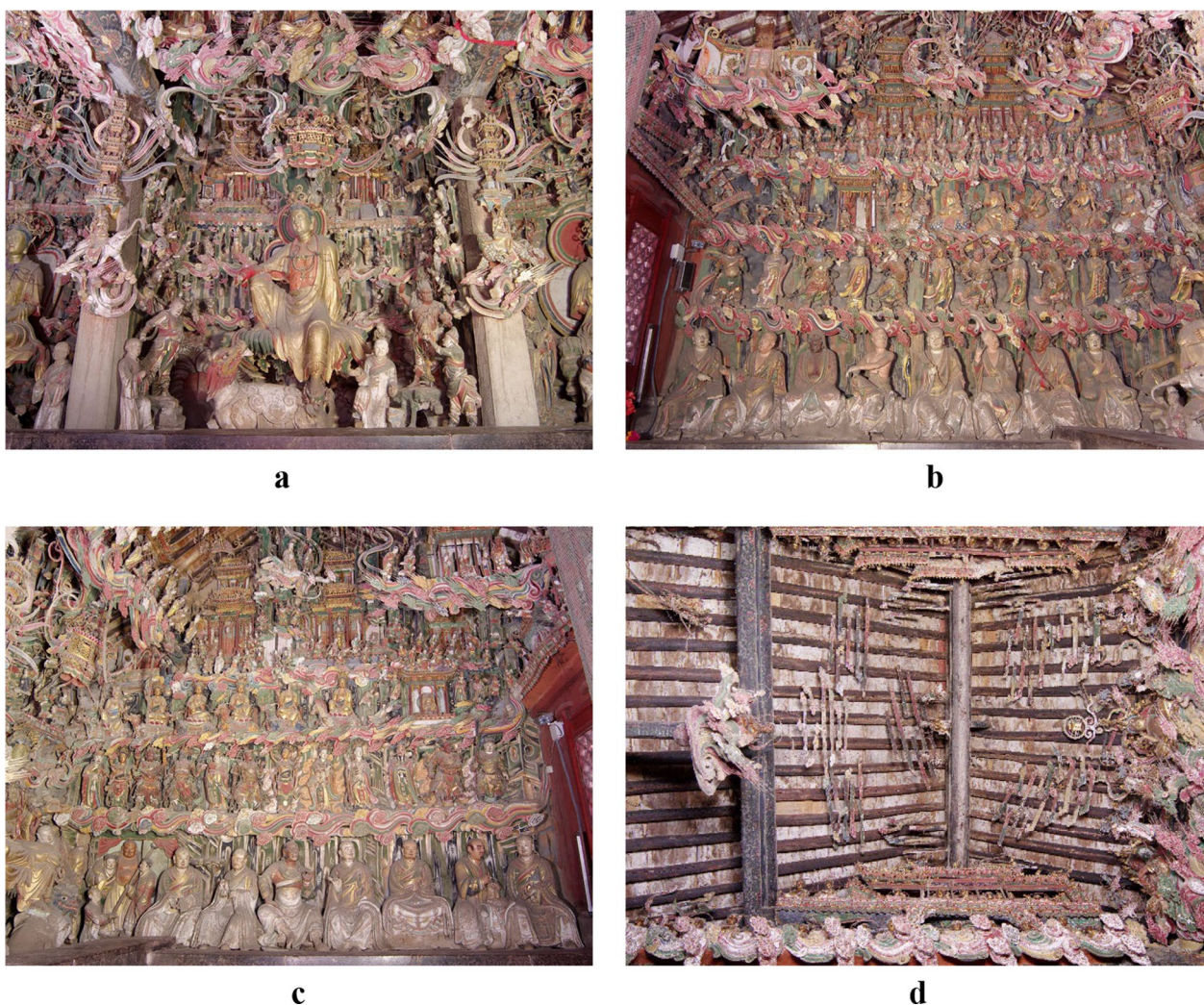


Fig. 1 Each wall of Guanyin Hall. **a** The western wall **(b)** The southern wall **(c)** The northern wall **(d)** The ceiling

platforms for support. Conversely, hanging sculptures, featuring smaller dimensions, are suspended from walls or roofs via wooden supports and nails. In addition to the strong cultural and historical background of Guanyin Hall, its value also lies in its exquisite art of hanging sculptures. More than 1000 sculptures of gods are found in the small hall because most of the statues are hanging sculptures. Hanging sculptures are vivid, three-dimensional art forms often used in temples to create complex backgrounds for storytelling scenarios. The upper body of the sculpture is slightly tilted outward, and the lower body blocks the upper feet when overlapping, creating a stunning effect after overlapping the upper and lower layers.

As depicted in Fig. 2, the painted sculptures within Guanyin Hall exhibit varying degrees of deterioration due to their unique structural design and poor preservation conditions. The severity of these issues includes instances of sculptures falling, missing clay, salt efflorescence and pigment layer detachment. Addressing these concerns promptly requires the implementation of scientific conservation measures. The current research surrounding the painted sculptures of Guanyin Hall predominantly revolves around cultural and artistic aspects, with limited exploration into their production processes, preservation and restoration techniques [4]. Complicating matters further, the production methods for painted sculptures across distinct periods and regions vary considerably. Consequently, existing research outcomes fail to offer substantial guidance or reference points. A substantial void exists in terms of scientifically credible evidence corroborating the materials and procedures employed in crafting the painted sculptures of Guanyin Hall.

The integration of various modern analytical methods has proven to be a powerful approach for material identification and characterisation. X-ray photography is a well-established method of non-destructive analysis that can be used to explore the internal structure and details of cultural relics [5]. The combination of scanning electron microscopy with energy dispersive spectrometer analysis and X-ray diffractometer has been instrumental in identifying pigments [6, 7]. Additionally, the application of a mineral liberation analyser provides a highly accurate method of determining the content of various components of clay [8]. As a well-developed technique, granulometric analysis has been effectively used for examining the particle sizes of clay samples [9]. Furthermore, the combined use of various stains and an optical microscope has been successful in distinguishing wood and plant fibre sources [10, 15]. In the scope of this work, an array of analytical techniques, were employed to delineate the production process and assess the preservation status of sculptures. The conclusions derived from

these analyses furnish dependable substantiation that can guide future preservation and restoration endeavours.

Materials and methods

Non-destructive sampling was impossible due to the comprehensive preservation of the placement sculptures within Guanyin Hall [11]. Therefore, this study predominantly focuses on the analysis and investigation of the small hanging sculptures. In this paper, a total of 19 samples from six categories were tested. The internal structure of five complete hanging sculptures (XS-1–5) was analysed nondestructively. The mineral composition and particle size distribution of four clay fragments (ST-1–4) were characterised. Species identification of two wood (MC-1–2) and two plant fibre (XW-1–2) samples was performed. The composition and process of two iron wire samples (TS-1–2) were also analysed. The raw materials of six pigment samples (YL-1–6) were determined. The collected samples are detailed in Table 1. Amongst them, samples XS-1–5 and ST-1–4 were selected from dropped sculptures and debris in the display case, samples XW-1–2 were separated from ST-1–4 and the sources of the remaining samples are shown in Fig. 3.

X-ray test

A non-destructive approach was employed to analyse the internal structure and potential problems of the dropped complete hanging sculptures (XS-1–5) using an X-ray real-time image system (manufactured by Dandong Industrial NDT Equipment Factory, China). This system operated at a shooting voltage of 80 kV, a current of 5 mA, an exposure time of 80 s and a distance of 80 cm [12].

Microscope analysis

A digital microscope (Keyence VHX-2000C, Japan) was used to observe the microscopic morphology of the cross-section of samples ST-1–2 and the surfaces of ST-3–4 and obtain information on the fabrication process. Samples ST-1–2 were embedded with epoxy resin and then sanded and polished, whilst samples ST-3–4 were directly observed after cleaning the surface.

An optical microscope (CaiKon DFM-66C, China) was used to identify the raw material species of plant fibres of clay fragments (XW-1–2) and wooden sticks (MC-1–2) of sculptures.

The wooden stick preparation process entailed several steps: softening involved placing the sample in a heated water bath at 85–90 °C, with periodic (30 min) transfers to cold water until sinking was realised. Reinforcement included immersing the sample and chopped paraffin wax in a container, subjecting it to a vacuum heating process at 70 °C, –0.08 MPa pressure and a 20 min



Fig. 2 Various diseases of clay sculptures. **(a)** Salt efflorescence **(b)** Warping of the paint layer **(c)** Peeling off of the paint layer **(d)** Fracture **(e)** Missing of clay **(f)** Falling of sculptures **(g)** Accumulating dust **(h)** Biological disease

Table 1 Information of the samples

Sample no	Image of the sample	Description
XS-1		Complete sculptures
XS-2		
XS-3		

Table 1 (continued)

Sample no	Image of the sample	Description
XS-4		
XS-5		
ST-1		Clay fragments of sculpture's surface
ST-2		

Table 1 (continued)

Sample no	Image of the sample	Description
ST-3		Clay fragments of sculpture's inside
ST-4		
MC-1		Wooden stick of sculpture's neck
MC-2		Wooden stick of sculpture's back
XW-1		Plant fibers of ST-3
XW-2		Plant fibers of ST-4

Table 1 (continued)

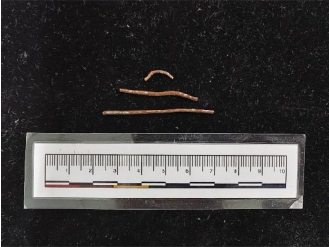
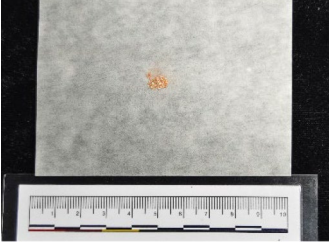
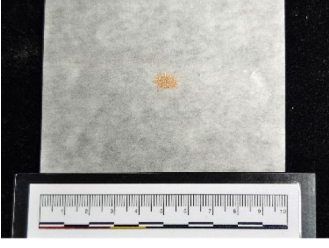
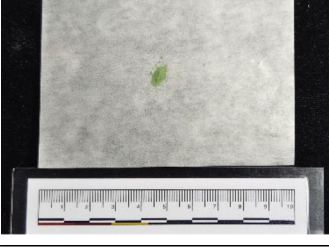
Sample no	Image of the sample	Description
TS-1		Iron wire of sculpture's arm
TS-2		Iron wire of the lower hem of sculpture's gown
YL-1		Red pigment
YL-2		Red pigment
YL-3		Pink pigment
YL-4		Green pigment

Table 1 (continued)

Sample no	Image of the sample	Description
YL-5		Cyan pigment
YL-6		Golden pigment

duration. Slicing encompassed the use of a slicer to cut transverse and tangential sections with a thickness of 15–25 μm . De-waxing was accomplished by melting paraffin wax from the slices using heated slides. Staining was performed using a 1.0% aqueous solution of saffron for 1–2 min. Dehydration included rinsing samples with a 50% aqueous alcohol solution, repeated 3–5 times. Sealing involved applying a drop of neutral gum onto slides with coverslips for observation under a light microscope [13].

Plant fibre samples were washed with distilled water, placed in a clean test tube and then subjected to ultrasonic shaking for dispersion. A small amount of fibres was then placed on a slide, stained using Herzberg's (I2-ZnCl₂) solution, covered with a coverslip and observed under a light microscope [14]. Various fibres exhibit distinct colours following Herzberg staining. When coupled with comprehensive fibre characteristics, this staining technique aids in the identification of fibre types [15].

MLA analysis

An MLA (FEI MLA650, America) was employed for quantitative mineral composition determination in clay fragment samples (ST-1–4). The process involved pulverising and purifying the clay samples, followed by epoxy resin cold embedding. Once the resin cured, sheets were crafted, ultrasonically cleaned in ethanol for 15 min, dried and treated with vapour-plated carbon film [16].

Laser particle size test

A laser particle size distributor (Bittersize BT-9300S, China) was utilised to assess particle size and distribution in clay fragment samples (ST-1–4). A 0.5% (NaPO₃)₆-H₂O solution was used for dispersion after grinding and sieving. The dispersed clay samples were subjected to laser particle size analysis through a recirculating dispersion feeding system, repeating the process three times for an averaged result.

Ion chromatography analysis

Soluble salt species and content in clay fragment samples (ST-1–4) were determined using an ion chromatograph (Dionex ICS-3000, America). Samples were dissolved in deionised water, ultrasonicated (5 min) and then centrifuged (4000 r/min for 10 min). The supernatant was filtered through a 0.22 μm microporous filter membrane.

XRF analysis

A handheld XRF analyser (SciAps X-200, America) in alloy mode with a 50 kV voltage setting was employed to ascertain the metal composition of iron wire samples (TS-1–2).

XRD analysis

A theta rotating anode XRD (Rigaku TTR-III, Japan) was used to analyse the composition of mineral pigment samples (YL-1–5) under the following conditions: Cu-K α tube, a voltage of 40 kV, a current of 200 mA and a continuous scanning range of 5 to 70°. A total of 3–4 mg of pigment sample was scraped off from the centre of the



Fig. 3 Sampling Locations. **a, b** Pigment and iron wire location **c, d** Wooden stick location

single crystal silicon plate, and a small amount of anhydrous ethanol was dropped to dissolve the adhesive wrapped around the pigment particles. The pigment will adhere to the sample plate after the ethanol evaporates. The monocrystalline silicon wafer sample plate containing the sample was inserted into the sample holder of the diffractometer for testing [17].

SEM-EDS analysis

Scanning electron microscopy with energy spectroscopy (Gemini SEM 500, Germany) was employed to establish the elemental composition of pigment samples (YL-1–6). Samples were analysed with a 20 kV acceleration voltage and 10 mm working distance. The results were combined with XRD outcomes to identify pigment species.

The samples (YL-1–5) were treated with Pt spray (YL-6 carbon spray treatment) for 275 s to enhance electrical conductivity. Afterwards, the samples were placed under the equipment for observation of their topographic characteristics and qualitative analysis of their elemental composition.

Results and discussion

Analysis of the complete clay sculptures

The X-ray images in Fig. 4 reveal that the five complete hanging sculptures have no full-body skeletons but incorporate a minimal amount of wire. This wire is specifically positioned in certain areas, such as flowing cuffs, lower gown hems and arms with large-amplitude movement, providing localised reinforcement to withstand substantial forces. Clay is soft when wet and does not support itself; therefore, a skeleton is necessary to support the clay when moulding. The skeleton includes full-body and partial skeletons, and the choice of skeleton material and size determines the quality and beauty of the sculpture. The space of a small hanging sculpture body is limited, and ensuring thin wooden skeleton strength is difficult. Therefore, an iron wire with high strength and ductility must be chosen.

Notably, the transition from the interior of the sculpture to its surface lacks distinct layering, whilst uniform small cracks are present within the sculpture, possibly due to clay shrinkage during the drying process. These cracks exhibit uniformity in length and distribution, presumably indicating the use of consistent clay materials. Furthermore, the sculptures display holes approximately 6–8 cm deep in their necks and feet. Neck holes accommodate wooden sticks for connecting and securing the body and head, whilst foot holes facilitate iron nail insertion for wall hanging (Fig. 5).

Analysis of the clay fragments

Microscopic images presented in Fig. 6 reveal two surface structure patterns characterised by varying thicknesses of the white ash layer. Clay sculptures from the inside to the outside are generally ordered as coarse clay, fine clay, white ash and pigment layers. However, the Guanyin Hall hanging sculpture did not display coarse and fine clay layer demarcation. Clay, white ash and pigmented layer structures, respectively. Sample ST-1 displays a thin and uneven white ash layer, approximately 28–50 μm thick, whereas sample ST-2 showcases a thicker and more even white ash layer, spanning approximately 118–135 μm . Differences in surface preservation become evident, with ST-1 exhibiting extensive detachment and chalking of the pigment layer, whilst the pigment layer of ST-2 remains relatively intact. These layers have been made by different artisans or in different batches, possibly due to variations

in materials and processes, leading to differences in the current state of preservation. The clay fragments were reinforced using two distinct fibre types: ST-3 features thin and dense fibres that enhance clay consolidation and toughness, whilst ST-4 incorporates short, thick and sparse fibres suspected to be wheat straw. ST-4 exhibits inferior consolidation and low clay strength.

Figure 7 illustrates the particle size distribution pattern of samples ST-1–4, revealing predominant particle sizes between 1 and 75 μm . Approximately 25–29% of clay grains are below 0.005 mm, whilst the largest proportion ranges from 0.005 to 0.075 mm (67–71%), and sand grains from 0.075 to 0.25 mm account for 3–5%. This clay predominantly comprises powder grains, with a proportion of clay grains added to enhance cohesion and plasticity, along with a marginal quantity of sand grains for increased mechanical strength and weathering resistance. The average particle size of soils from the Loess Plateau in the Shanxi Region of China is generally 50–70 μm [18], and the relatively uniform particle size and fine texture suggest meticulous sieving during production. These results confirm the high quality of clay used in sculpture creation.

Mineral analysis outcomes (Tables 2, 3) indicate comparable composition ratios between samples from different locations, with a slight disparity in kaolinite content attributed to potential hand-made variations. The primary components of the clay are quartz and biotite, constituting over 55% of the clay, alongside trace amounts of albite, chlorite, feldspar and kaolinite. Comparisons between interior and surface clay layers demonstrate similar particle size distributions and composition ratios. Combined with X-ray imagery, this finding implies that small hanging sculptures employed a single proportion of fine clay, differing from medium and large sculptures, which have coarse and fine layers.

Ion chromatography results (Table 4) indicate a substantial impact of soluble salts on the sculptures, with elevated concentrations of certain ions surpassing normal levels. Ca^{2+} , SO_4^{2-} and NO_3^- are notably abundant, and the order of binding activity suggests the presence of soluble salts such as CaSO_4 , NaCl and Na_2SO_4 , respectively. The SO_4^{2-} content in sculpture samples surpasses that of Cl^- , implying a considerable influence from soluble salts such as NaCl and Na_2SO_4 , which are known to affect soil cultural relics [19]. Na_2SO_4 is hypothesised to play a pivotal role in salt efflorescence disease within Guanyin Hall sculptures. Moreover, soluble salt concentrations are remarkably higher in surface samples, implying a gradual migration from the interior to the exterior of sculptures. The soluble salts originate from the clay itself and the accumulated dust in the air; the latter will adsorb the airborne salts, organic matter and bacterial

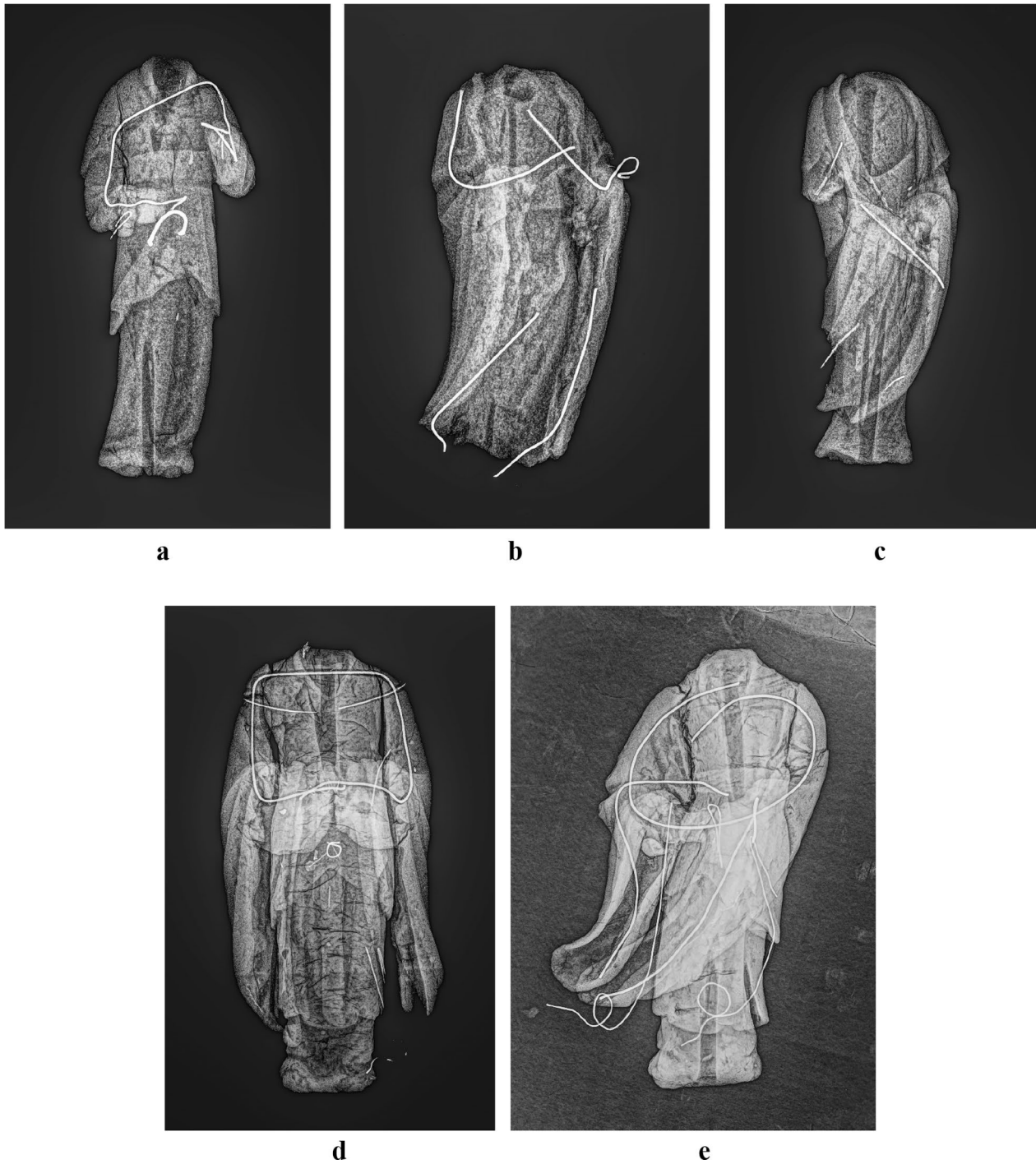


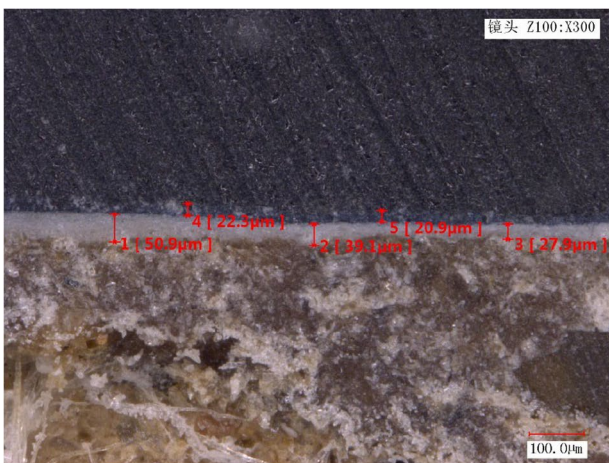
Fig. 4 X-ray images of complete clay sculptures. **a** XS-1 **(b)** XS-2 **(c)** XS-3 **(d)** XS-4 **(e)** XS-5

moulds deposited on the surface of the sculpture. Environmental humidity and cyclic fluctuations facilitate salt and water penetration and accumulation, culminating in salt efflorescence, pigment layer warping and other issues. Organic matter fosters bacterial and mould

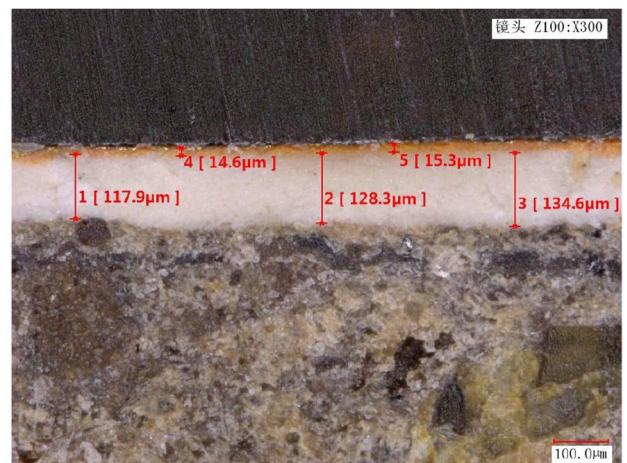
growth, leading to hollowing, pigment layer flaking, chalking and diminished clay strength, which can cause irreversible damage to cultural relics [20]. Each dry–wet cycle further damages the sculpture due to the lack of temperature and humidity control equipment. Warm and



Fig. 5 The hang of clay sculpture



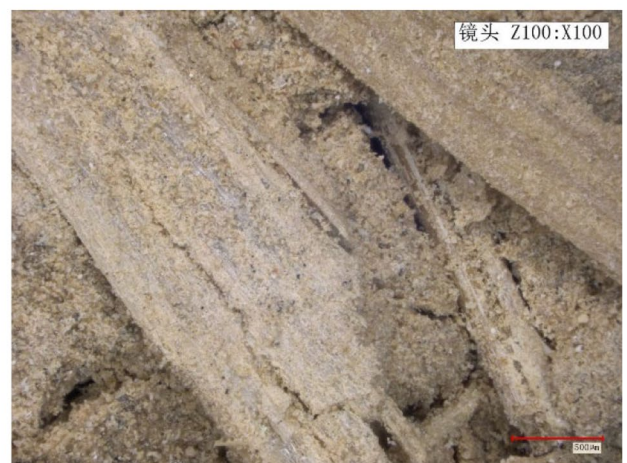
a



b



c



d

Fig. 6 Cross section microscopic images of clay fragments. **a** ST-1 (**b**) ST-2 (**c**) ST-3 (**d**) ST-4

humid air carries pollutants; when combined with soluble salts and micro-organisms in the dust, condensation can occur on the surface as well as in the interior, which is prone to mould growth and microbial contamination [21]. The condensed water evaporates and the soluble

salts crystallise as the humidity decreases, leading to diseases such as salt efflorescence, weathering, warping and flaking of the pigment layer, further threatening the strength of the sculpture [22]. Dust also contains acidic and alkaline chemical particles, metal dust and microbial

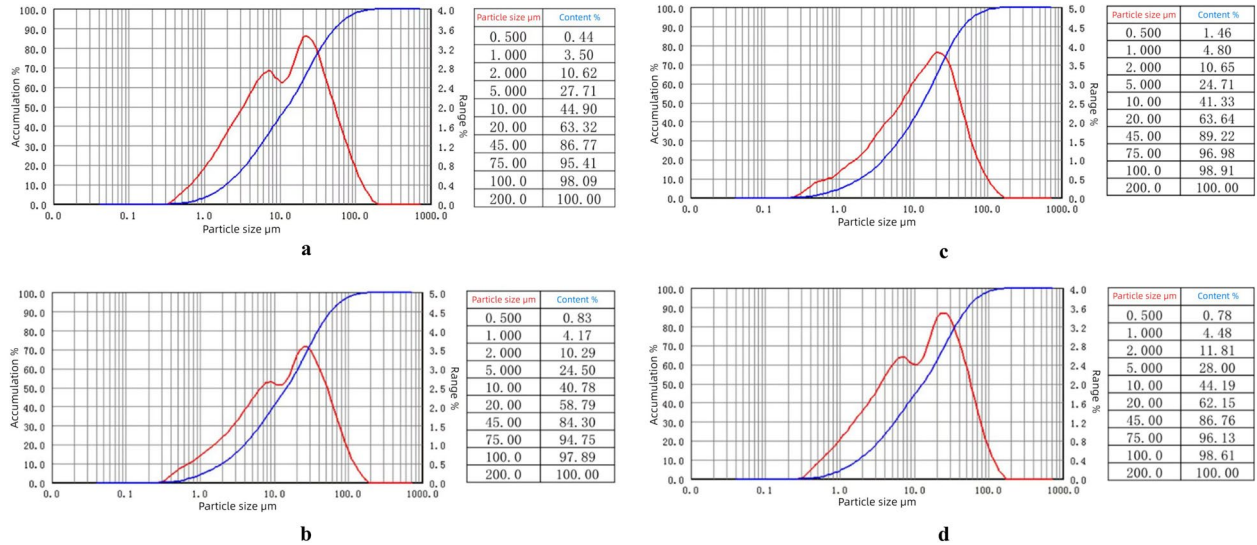


Fig. 7 Results of granulometric analysis. **a** ST-1 **(b)** ST-2 **(c)** ST-3 **(d)** ST-4

Table 2 Mineral analysis results (surface)

Mineral	Weight percent	Area percent	Area (μ ²)	Segment number	Relative error
Quartz	30.32	28.7	1,159,804	6717	0.02
Biotite	30.08	28.44	1,149,324	9259	0.02
Albite	9.37	8.86	358,092.6	2013	0.04
Chlorite	7.8	8.09	326,980.3	2815	0.04
Feldspar	7.23	7.13	288,055.1	1819	0.05
Kaolinite	5.41	5.22	210,899	1872	0.05
Anorthite	3.01	2.92	117,893.4	989	0.06
Calcite	1.09	1.02	41,336.53	283	0.12

Table 3 Mineral analysis results (inside)

Mineral	Weight percent	Area percent	Area (μ ²)	Segment number	Relative error
Quartz	29.23	27.63	1,197,498	6380	0.02
Biotite	26.7	25.14	1,089,274	7785	0.02
Albite	9	8.5	368,171	1802	0.05
Chlorite	8.29	8.66	375,312.3	2979	0.04
Kaolinite	7.35	7.05	305,475.8	2387	0.04
Feldspar	7.1	6.98	302,524.5	1661	0.05
Anorthite	2.71	2.6	112,767.1	911	0.07
Calcite	1.27	1.2	51,839.57	299	0.12

Table 4 Soluble salt results

Sample	Content($\mu\text{g}/\text{mL}$)						
	Cation				Anions		
	K^+	Na^+	Ca^{2+}	Mg^{2+}	Cl^-	NO_3^-	SO_4^{2-}
ST-1	3.46	2.61	189.65	2.47	4.89	5.75	589.1
ST-2	2.82	4.93	113.38	2.53	9.23	19.03	290.6
ST-3	7.31	9.24	75.45	3.43	3.99	5.02	141.0
ST-4	4.49	9.79	82.26	4.93	8.53	13.41	172.0

spores. Dust accumulation on the cultural relics will not only change the appearance of colour and affect the formation of a dirt layer but also induce chemical corrosion and mechanical damage. The aforementioned factors on the impact caused by painted sculptures are not single physical factors but are a combination of physical, chemical and biological factors such as the synergistic effect of the results. This synergistic effect seriously damages painted sculptures and even the entire building [23].

Analysis of the wooden sticks and plant fibers

The microscopic image (Fig. 8) shows that the cross-section of sample MC-1 is sharply changed from earlywood to latewood, with normal resin canals. The wood rays in the tangential section exhibit uniseriate and fusiform rays, and the uniseriate rays were 4–12 cells high. The fusiform rays had radial resin tracts, and 2–3 rows of ray cells were observed above and below the resin tract. Both ends are pointed and single row, approximately 9–10 cells high. The inner wall of the ray tube cells is smooth and slightly serrated. These characteristics are consistent with the attributes of Pinaceae wood. Considering the resin tracts, fusiform rays and geographical distribution, further analysis suggests that the raw material comes from pine or larch wood within the Pinaceae family.

The cross-section of sample MC-2 is characterised by scattered pores. The conduits have single pores and 2–5 short-diameter rows of compound pores and the pores are very small (the single pores are less than $1\ \mu\text{m}$). A few of these pores have polygonal profiles, and the rest of the characteristics are not observed due to the extrusion by the paraffin filler. The axial parenchyma of the tangential section is scattered; wood rays are non-stacked with uniseriate rays, approximately 15–18 cells high; crystals and gum are absent; and the wood grain has a straight and fine structure. The above characteristics are consistent with those of the wood of the genus *populus* [24]. Thus, the raw material is the wood of the genus *populus* in the family of *populus*.

Pine and *populus* are both common woods in northern China and are easily accessible. Both woods are tough and strong; they are also easy to cut and process due to

their moderate hardness. In addition, pine and poplar are highly resistant to corrosion, with pine itself containing natural compounds such as rosin and turpentine, which further enhance its anticorrosive and antibacterial capabilities.

The microscopic image presented in Fig. 9 illustrates the characteristics of the analysed fibres. Sample XW-1, which underwent Herzberg staining, appears light brown with a wine-red hue. The fibres exhibit a cylindrical shape with noticeable transverse lines on the fibre wall. These lines are inclined at a certain angle relative to the cross-section. An outer transparent membrane is visible on the fibre's surface, and some parts of this membrane appear semi-detached due to beating, thereby forming a wrinkle-like pile. Additionally, certain fibres contain cell cavities within their middle, manifesting as light-coloured lines. The interspaces between the fibres are occupied by square parenchyma cells and calcium oxalate crystals, aligning with the typical morphological characteristics of mulberry fibres [25].

In the case of sample XW-2, Herzberg staining results in a dark blue/violet colour. The sample displays libriform fibres and tracheid cells. The libriform fibres are straight, fine and pointed, featuring transverse lines on their surfaces and a narrow cell lumen. By contrast, the tracheid cells are wider with blunt ends. Their surface is also smooth, possessing a thin fibre wall and a wide cell lumen. Furthermore, the interspaces between these fibres contain rectangular, thin-walled cells with serrated epidermal cells. These characteristics are consistent with the morphological traits of wheat straw fibres [26].

Wheat straw was widely used in ancient China for murals and clay sculptures to enhance the mechanical strength of the clay [27]. When chopped, wheat straw is mostly in the form of thin flakes with a large surface area, allowing its close adherence to the soil, whilst its inherent high strength makes it an ideal reinforcing material. Notably, examples of the application of structural bark fibres in clay sculpture have not been found. However, microanalysis results show that the fibre size is consistent and uniformly stained, almost free of impurities such as thick fibres and surface coarse bark, increasing the

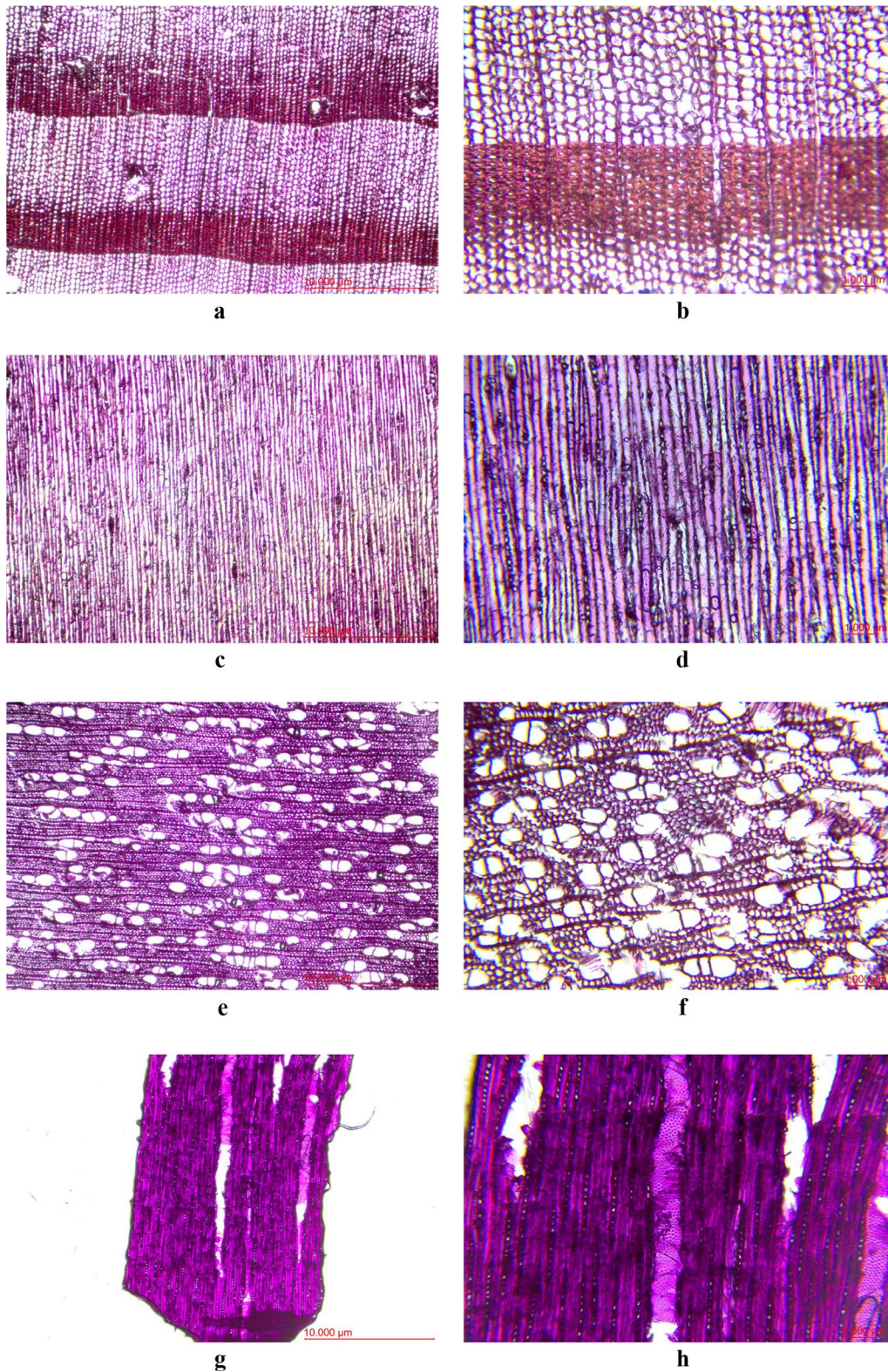


Fig. 8 Microscopic images of wooden sticks. **a, b** cross section of MC-1 (**c, d**) tangential section of MC-1. **e, f** cross section of MC-2 (**g, h**) tangential section of MC-2

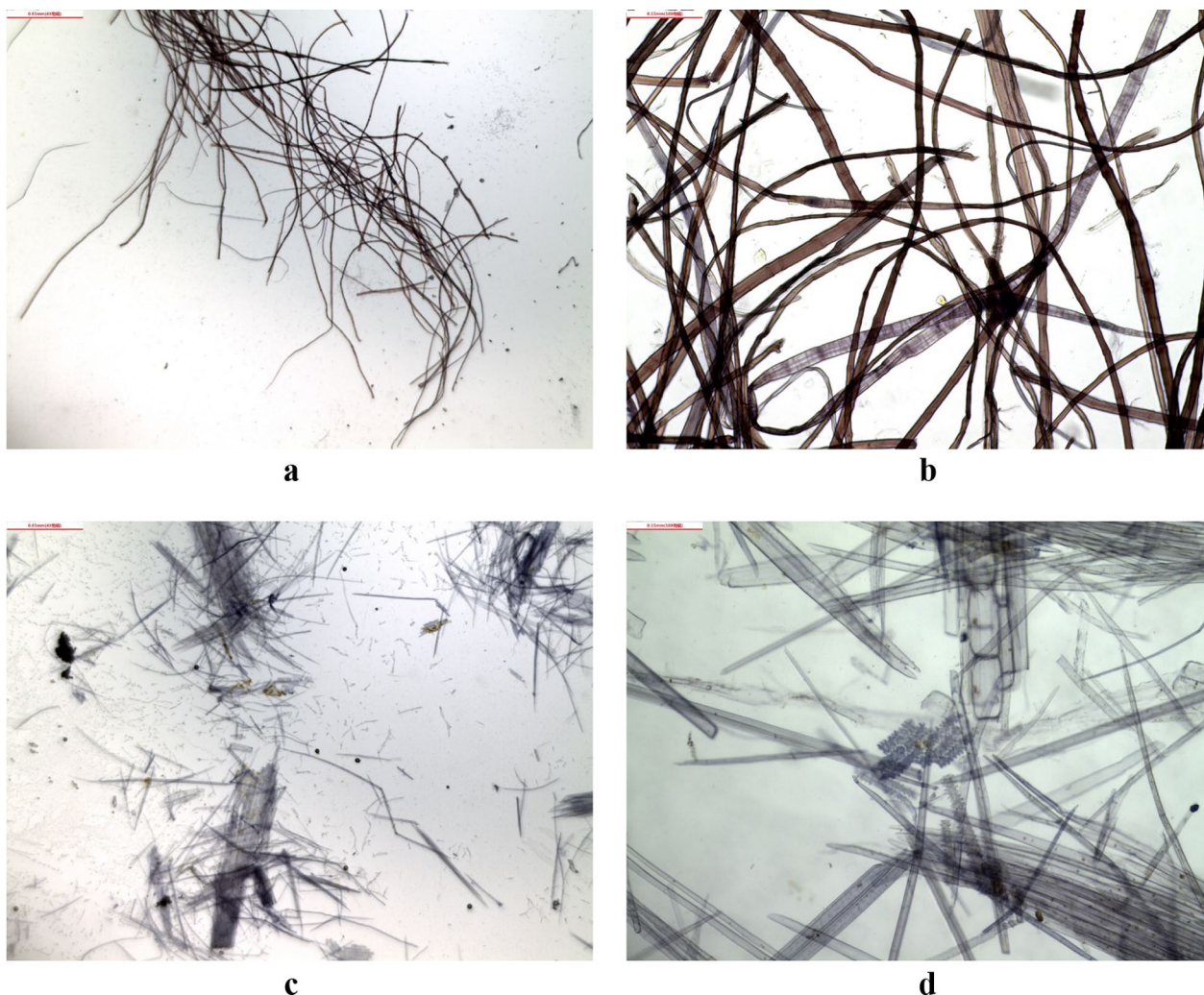


Fig. 9 Microscopic images of plant fibers. **a, b** XW-1 (**c, d**) XW-2

difficulty of the fibre treatment process. During statue formation, the high-grade mulberry paper was assumed to be soaked and broken up directly to obtain pulp, which was then mixed into the clay for production. A similar process has been followed in the Yuan Dynasty mural production [28].

Analysis of the iron wires

The XRF analysis results presented in Table 5 indicate that the sample comprises pure iron with minimal carbon content. The metallographic structure of the sample (Fig. 10) predominantly comprises ferrite, along with a small proportion of spherical pearlite. This finding suggests that the sample likely comprises annealed wrought iron. Notably, an extrusion deformation phenomenon is observed in the ferrite at the edge of the sample's cross-section metallographic structure. This phenomenon may

be attributed to a drawing or extrusion process [29]. The Ancient Chinese iron wire production method is a drawing process, precisely because of the high hardness and toughness of iron. This process also matured later. The drawing process appeared in the Song Dynasty, until the Ming Dynasty had a greater development. According to ancient records, at that time, Zhejiang, Shanxi, Guangdong and other places had iron wire production. The purity and precision of the iron wire used in the Guanyin Hall hanging sculpture are extremely high, the finest of which is less than 1 mm in diameter, reflecting the high standard and scientific nature of the material selection.

Analysis of the pigments

The XRD results in Fig. 11 show that the Si_2O and $\text{Al}_2\text{Si}_2\text{O}_5(\text{OH})_4$ contained in samples YL-1–5 correspond to quartz and kaolinite, which have been detected

in mineral analysis and can be considered impurities in pigment analysis. HgS , Pb_3O_4 and Fe_2O_3 were detected in the red pigment samples (YL-1, 2), suggesting that the red pigments of the sculpture were cinnabar, red lead and iron red, respectively. Different red pigments were possibly chosen for mixing to present a variety of colours. In addition, As_4S_4 was found in the pink pigment (YL-3), and PbCO_3 white pigment was detected. The red pigment realgar was possibly mixed with cerusite during production to obtain the pink colour effect. The use of a mixture of multiple pigments to obtain different colours was a common technique in the production of clay sculptures and murals in ancient China [30, 31]. In the green pigment sample YL-4, atacamite $[\text{Cu}_2\text{Cl}(\text{OH})_3]$ and brochantite $[\text{Cu}_4\text{SO}_4(\text{OH})_6]$ were detected, but the latter content was substantially small; therefore, the main component of the green pigment is atacamite [32]. XRD patterns suggested that brochantite $[\text{Cu}_4\text{SO}_4(\text{OH})_6]$ and azurite $[\text{Cu}(\text{OH})_2(\text{CO}_3)_2]$ were the primary crystalline phases in the sample YL-5. Similarly, cyan pigments are made by mixing green and blue pigments. The SEM–EDS results (Table 6) further corroborate the conclusions of the XRD, which detected the corresponding elements in the pigment compositions, identifying the source of the mineral pigments used in the sculptures. Simultaneously,

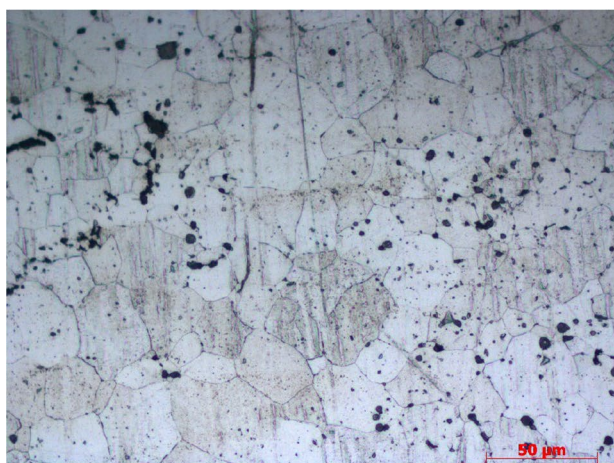
the above pigment samples were covered by pollutant minerals (mainly from dust), which caused the detection of elements such as Si and Al in the samples [33]. YL-6 contains a substantially high amount of Au and was processed using a technique involving spraying C, further increasing the corrected Au content. This finding suggests that the sample comprises a gold foil made from pure gold. Gilding is a traditional craft that was widely used in ancient China and Europe for sculptures [34–36]. Gold foil is attached to the surface of the sculpture's costume, reflecting the splendour and majesty of the statue.

Conclusions

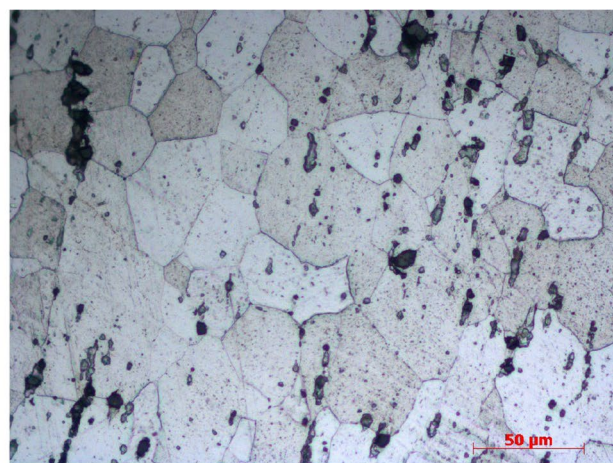
The painted sculptures in Guanyin Hall display intricate artisanship and carefully selected materials. The production process demonstrates adaptability and innovation, departing from tradition to suit specific size, hanging method and artistic style requirements. The small hanging sculptures have only a partial skeleton made of wire and comprise one type of clay, meticulously processed from loess with added sand for enhanced weather resistance. Two types of plant fibres, namely mulberry and wheat straw, were employed for reinforcement, each offering distinct concretion effects. Thin and long mulberry fibres bolstered clay block strength, whilst

Table 5 XRF results

Sample	Analyte (%)						
	Fe	Si	Cl	P	Ca ⁻	K	Sn ⁻
TS-1	94.2352	2.4906	1.9552	0.5841	0.4190	0.3158	
TS-2	98.7219				0.2002	0.2776	0.8003



a



b

Fig. 10 Metallographic micrograph of iron wires. **a** TS-1 **(b)** TS-2

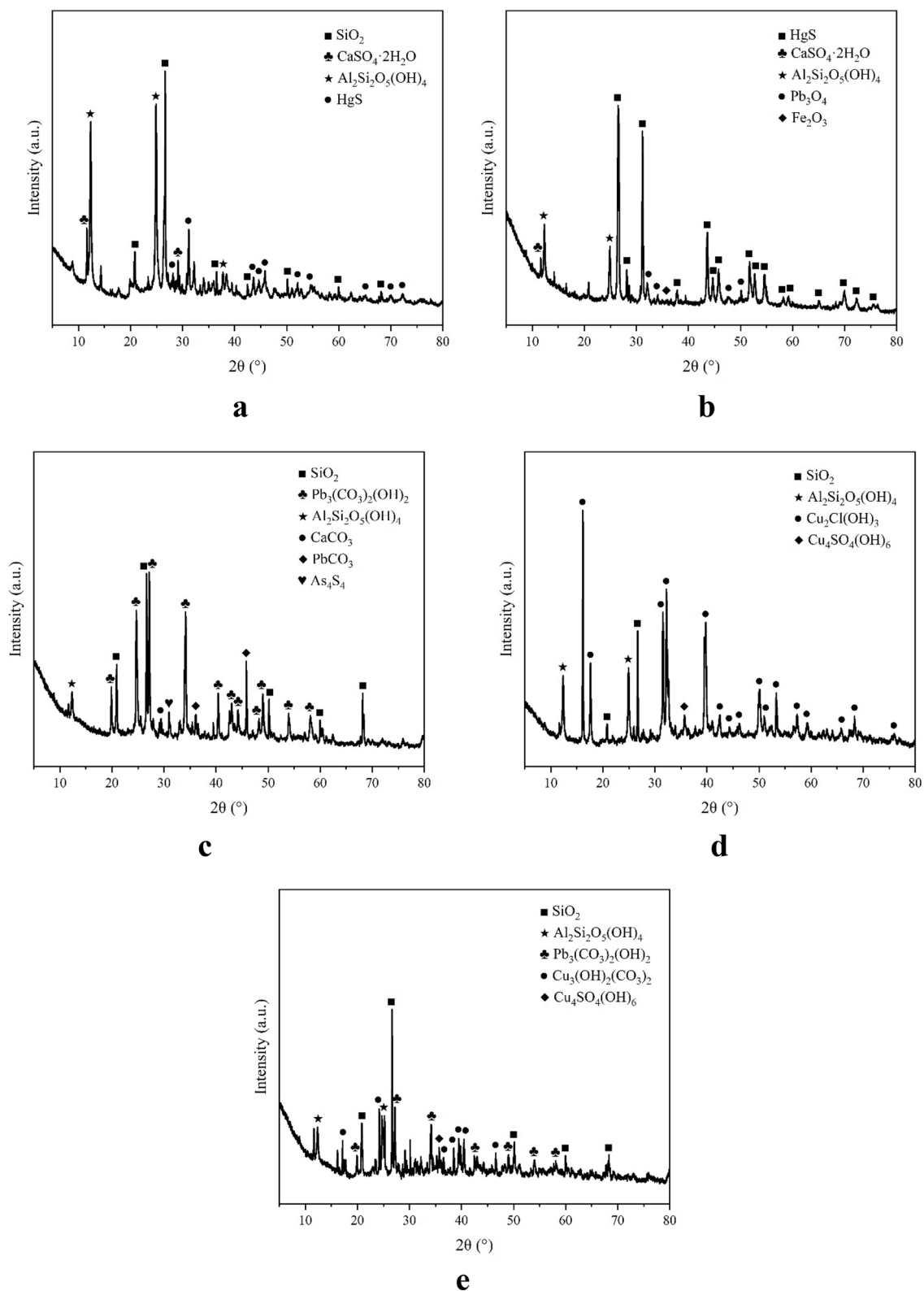


Fig. 11 Results of X-ray Diffractometer. **a** YL-1 **(b)** YL-2 **(c)** YL-3 **(d)** YL-4 **(e)** YL-5

Table 6 Results of SEM–EDS

Element	C	O	Na	Al	Si	S	Cl	Ca	Cu	Pb	Au	Ag
YL-1	26.26	21.51		6.85	8.19	11.36	1.67	19.73		6.34		
YL-2	24.78	15.82		1.03	0.81	4.87	4.16	14.97		33.56		
YL-3	9.97	49.87	1.16	7.58	8.71	5.29	1.76	9.88	1.63	4.15		
YL-4	31.32	17.66		2.44	2.23	1.27	10.55	3.35	24.38			
YL-5	28.72	16.59		3.26	2.63		8.10	1.72	20.15	18.83		
YL-6	30.77	11.98		1.08				1.79	0.73	2.89	46.36	4.40

short and thick wheat straw fibres were only slightly effective. The clay is mixed with the reinforcing material and then thoroughly stirred and pounded to exhaust the air. Afterwards, the clay is moulded into a preliminary shape, with an additional small amount of fine wire to support some unusual parts. Wooden sticks of suitable size made of pine wood were used to connect the body and head at the neck, and a few sculptures were supported by wooden sticks made of populus wood on the back, which were presumed to be used for the support or hanging of a few sculptures located in special positions because no sculptures of the same kind could be found to confirm their function. Meanwhile, most of the hanging sculptures were hung on the wall by inserting iron nails into the feet. The sculptures underwent a process of drying, carving, polishing and coating with a white ash layer before their decoration with traditional mineral pigments such as cinnabar, red lead, iron red, cerussite, atacamite, brochantite and azurite, and even gold foil for gold painting, which is a rare technique in folk temple sculptures.

Overall, the painted sculptures of Guanyin Hall are invaluable cultural relics representing local religious artistry. However, their deteriorating condition necessitates urgent conservation and restoration efforts. Employing various analytical techniques, this study provides vital insights into the materials, production processes and problems of sculptures. The findings offer reliable guidance for restoration material selection and preservation strategies, shedding light on the challenges posed by various physical, chemical and biological factors that contribute to the degradation of sculptures. The synergistic impact of these factors exacerbates the deterioration, emphasising the urgency of comprehensive preservation measures to safeguard these precious heritage pieces and their cultural legacy.

Acknowledgements

We are thankful to Cultural Relics Management Office of Guanyin Hall for providing the samples. The technical support from Experimentation Center for Physical Science, University of Science and Technology of China is greatly appreciated.

Author contributions

BZ performed the examination, analyzed and interpreted the data, and was a major contributor in writing the manuscript. CQ and DY assisted in performing the experiments. DG provided the experimental ideas. YG supervised the entire research procedures. All authors read and approved the final manuscript.

Funding

There is no funding supported for this research.

Availability of data and materials

All data generated or analyzed during this study are included in this article.

Declarations

Competing interests

The authors declare that they have no competing interests as defined by Springer, or other interests that might be perceived to influence the results and/or discussion reported in this paper.

Author details

¹Department for the History of Science and Scientific Archaeology, University of Science and Technology of China, 96 Jinzhai Rd, Hefei, People's Republic of China. ²Department for the History of Science, Jiangsu University of Science and Technology, 666 Changhui Rd, Zhenjiang, People's Republic of China.

Received: 14 August 2023 Accepted: 3 December 2023

Published online: 02 January 2024

References

- Yang B, Zhou RC. Study on the conservation of painted sculptures of Guanyin hall Changzhi. *J Chin Antiquity*. 2019;01:48–52 (In Chinese).
- Jiang S. Gathering of the Spirits- Liangjiazhuang Guanyin Hall. *Beiyue Literature & Art Publishing House*; 2014. P. 37–38. (In Chinese)
- Jiao MR. Conservation and analysis of painted sculptures of guanyin hall, Changzhi. *Identificat Appreciat Cultur Relics*. 2021;14:142–4 (In Chinese).
- Guo JL. Aesthetic analysis of painted sculpture of the ming dynasty of Changzhi Guanyintang. *Art Design*. 2014;2(10):147–9 (In Chinese).
- Mannes D, Schmid F, Frey J, Schmidt-Ott K, Lehmann E. Combined neutron and x-ray imaging for non-invasive investigations of cultural heritage objects. *Phys Procedia*. 2015;69:653–60. <https://doi.org/10.1016/j.phpro.2015.07.092>.
- Egel E, Simon S. Investigation of the painting materials in Zhongshan Grottoes (Shaanxi, China). *Herit Sci*. 2013;1(1):29. <https://doi.org/10.1186/2050-7445-1-29>.
- Zhang YD, Wang JL, Liu HL, Wang XD, Zhang S. Integrated analysis of pigments on murals and sculptures in Mogao Grottoes. *Anal Lett*. 2015;48(15):2400–13. <https://doi.org/10.1080/00032719.2015.1038557>.
- He T, Sun YB, Gray J, Gu Y. Analysis iron distribution methods in fine sand- and silt-sized soil particles. *Methods X*. 2021;8:101248. <https://doi.org/10.1016/j.mex.2021.101248>.

9. Huang F. Research on the conservation of color-painted sculptures of the Tang dynasty of Foguang Temple in Wutai. M.A. dissertation: University of Science and Technology of China 2014. **(In Chinese)**.
10. Ruffinatto F, Cremonini C, Macchioni N, et al. Application of reflected light microscopy for non-invasive wood identification of marquetry furniture and small wood carvings. *J Cultural Heritage*. 2014. <https://doi.org/10.1016/j.culher.2013.11.013>.
11. ICOMOS China. Principles for the Conservation of Heritage Sites in China. Beijing: Cultural Relics Press; 2015. P. 10–15. **(In Chinese)**.
12. Xiang JK, Ma LY, Bai K, Dong SH, Zhang G. X-radiographic study of Liao Dynasty clay sculptures in Fengguo temple, Liaoning Province. *Sci Conserv Archaeol*. 2022;34(06):97–104. **(In Chinese)**.
13. Cartwright CR. The principles, procedures and pitfalls in identifying archaeological and historical wood samples. *Ann Bot*. 2015. <https://doi.org/10.1093/aob/mcv056>.
14. Giorgi R, Dei L, Schettino C, Baglioni P. A new method for paper deacidification based on calcium hydroxide dispersed in nonaqueous media. *Study in Conservation*. 2002;47(Supplement-3):69–73. <https://doi.org/10.1179/sic.2002.47.s3.014>.
15. Li T, Ji JX, Zhou Z, Shi JL. A multi-analytical approach to investigate date-unknown paintings of Chinese Taoist priests. *Archaeol Anthropol Sci*. 2017;9(3):395–404. <https://doi.org/10.1007/s12520-015-0293-9>.
16. Wilton D, Thompson GM, Lamswood DE. MLA-SEM characterization of sulphide weathering, Erosion, and transport at the Voisey's Bay Orthomagmatic Ni-Cu-Co Sulphide Mineralization, Labrador, Canada. *Minerals*. 2021;11:1224. <https://doi.org/10.3390/min11111224>.
17. Galván Josa V, Bertolino SR, Laguens A, et al. X-ray and scanning electron microscopy archaeometric studies of pigments from the Aguada culture, Argentina. *Microchem J*. 2010;96(2):259–68. <https://doi.org/10.1016/j.microc.2010.03.010>.
18. Shen JY, Li L, Zhang DD, Dong SH, Xiang JK, Xu N. A Multi-analytical approach to investigate the polychrome clay sculpture in Qinglian temple of Jincheng, China. *Materials*. 2022;15:5470. <https://doi.org/10.3390/ma15165470>.
19. Heiner S. Salt efflorescence as indicator for sources of damaging salts on historic buildings and monuments: a statistical approach. *Environ Earth Sci*. 2018. <https://doi.org/10.1007/s12665-018-7752-4>.
20. Wang XS, Wan L, Huang JZ, Cao WB, Xu F, Dong P. Variable temperature and moisture conditions in Yungang Grottoes, China, and their impacts on ancient sculptures. *Environ Earth Sci*. 2014;72(8):3079–88. <https://doi.org/10.1007/s12665-014-3213-x>.
21. Li TX, Cai YZ, Ma QL. Microbial diversity on the surface of historical monuments in Lingyan temple, Jinan, China. *Microbial Ecol*. 2022. <https://doi.org/10.1007/s00248-021-01955-w>.
22. Sheng L, Xie HR, Ma Y, Hokoi SC, Li YH. Assessing the deterioration risk of polychrome clay sculptures based on the hygrothermal environment: a case study of Baosheng temple China. *Case Stud Construct Mater*. 2022. <https://doi.org/10.1016/j.cscm.2022.e01287>.
23. Liang J, Deng D, Zhou X, Liu K. The ecosystem protection and promotion of Mogao Grottoes. *E3S Web of Conferences*. 2020, 199: 00010. <https://doi.org/10.1051/e3sconf/202019900010>.
24. Xu F, Liu HQ. Comparative wood identification charts. Chemical Industry Press; 2016. P. 6 202. **(In Chinese)**
25. Ilvessalo-Pfäffli, Marja-Sisko. Fiber atlas: identification of papermaking fibers. State University of New York: Springer Series in Wood Science; 1995. P. 292–298.
26. Shi JL, Li T. Technical investigation of 15th and 19th century Chinese paper currencies: fiber use and pigment identification. *J Raman Spectrosc*. 2013. <https://doi.org/10.1002/jrs.4297>.
27. Bai XJ, Jia C, Chen ZG, Gong YX, Cheng HW, Wang JY. Analytical study of Buddha sculptures in Jingyin temple of Taiyuan, China. *Herit Sci*. 2021. <https://doi.org/10.1186/s40494-020-00471-3>.
28. Li SP. Preliminary analysis of ancient Chinese mural painting production technology. *China Cultural Heritage Sci Res*. 2009;02:89–92. **(In Chinese)**.
29. DLGAQ Castillo. The metallography of medieval agricultural and quotidian iron utensils from the rural settlement of Zaballa (Basque Country). *Archaeometry*. 2018. <https://doi.org/10.1111/arc.12387>.
30. Chen XL, Xia Y, Ma YR, Lei Y. Three fabricated pigments (Han purple, indigo and emerald green) in ancient Chinese artifacts studied by Raman microscopy, energy-dispersive X-ray spectrometry and polarized light microscopy. *J Raman Spectrosc*. 2008;38(10):1274–9. <https://doi.org/10.1002/jrs.1766>.
31. He L, Wang N, Zhao X, Zhou T, Xia Y, Liang JY, Rong B. Polychromic structures and pigments in Guangyuan Thousand-Buddha Grotto of the Tang Dynasty (China). *J Archaeol Sci*. 2012;39(6):1809–20. <https://doi.org/10.1016/j.jas.2012.01.022>.
32. Li ZM, Wang LL, Ma QL, Mei JJ. A scientific study of the pigments in the wall paintings at Jokhang Monastery in Lhasa, Tibet. *China Herit Sci*. 2014;2:21. <https://doi.org/10.1186/s40494-014-0021-2>.
33. Liu L, Gong DC, Yao ZQ, Xu LJ, Zhu ZY, Eckfeld T. Characterization of a Mahamayuri Vidharajni Sutra excavated in Lu'an. *China Herit Sci*. 2019;7(1):1–9. <https://doi.org/10.1186/s40494-019-0320-8>.
34. Crina Anca Sandu I, Helena de Sá M, Costa Pereira M. Ancient, "gilded" art objects from European cultural heritage: a review on different scales of characterization. *Surf Interface Anal*. 2011;43:1134–51. <https://doi.org/10.1002/sia.3740>.
35. Wang N, He L, Egel E, Simon S, Rong B. Complementary analytical methods in identifying gilding and painting techniques of ancient clay-based polychromic sculptures. *Microchem J*. 2014;114:125–40. <https://doi.org/10.1016/j.microc.2013.12.011>.
36. Zhou ZB, Shen L, Wang N, Ren XX, Yang J, Shi YC, Zhang H. Identification of organic materials used in gilding technique in wall paintings of Kizil Grottoes. *Chem Sel*. 2020;5(2):818–22. <https://doi.org/10.1002/slct.201903688>.

Publisher's Note

Springer Nature remains neutral with regard to jurisdictional claims in published maps and institutional affiliations.

Submit your manuscript to a SpringerOpen® journal and benefit from:

- Convenient online submission
- Rigorous peer review
- Open access: articles freely available online
- High visibility within the field
- Retaining the copyright to your article

Submit your next manuscript at ► [springeropen.com](https://www.springeropen.com)